Invited Paper

Terahertz Metamaterial Devices

R. D. Averitt*[a], W. J. Padilla[b], H. T. Chen[c], J. F. O'Hara[c], A. J. Taylor[c], C. Highstrete[d], M. Lee[d], J. M. O. Zide[e], S. R. Bank[e], A. C. Gossard[e]
[a]Department of Physics, Boston University, Boston, Massachusetts 02215;
[b]Department of Physics, Boston College, Chestnut Hill, Massachusetts 02467;
[c]MPA-CINT, MS K771, Los Alamos National Laboratory, Los Alamos, New Mexico 87545;
[d]Sandia National Laboratories, P.O. Box 5800, Albuquerque, New Mexico 87185;
[e]Materials Department, University of California, Santa Barbara, California, 93106

ABSTRACT

Compared to the neighboring infrared and microwave regions, the terahertz regime is still in need of fundamental technological advances. This derives, in part, from a paucity of naturally occurring materials with useful electronic or photonic properties at terahertz frequencies. This results in formidable challenges for creating the components needed for generating, detecting, and manipulating THz waves. Considering the promising applications of THz radiation, it is important overcome such material limitations by searching for new materials, or by constructing artificial materials with a desired electromagnetic response. Metamaterials are a new type of artificial composite with electromagnetic properties that derive from their sub-wavelength structure. The potential of metamaterials for THz radiation originates from a resonant electromagnetic response which can be tailored for specific applications. Metamaterials thus offer a route towards helping to fill the so-called "THz gap". In this work we discuss novel planar THz metamaterials. Importantly, the dependence of the resonant response on the supporting substrate enables the creation of active THz metamaterials. We show that the resonant response can be efficiently controlled using optical or electrical approaches. This has resulted in the creation of efficient THz switches and modulators of potential importance for advancing numerous real world THz applications.
Keywords: metamaterials, negative index, terahertz, far-infrared, time domain, ultrafast, femtosecond

1. INTRODUCTION

Electromagnetic metamaterials have experienced enormous excitement and growth recently due to the demonstration of exotic effects such as invisibility cloaking [1, 2], negative refractive index [3, 4], and perfect focusing [5]. In fact metamaterials offer an electromagnetic response which has been shown to be impossible to achieve in naturally occurring materials. Metamaterials are artificial structures which are fabricated to yield a designed resonant response to electromagnetic radiation. Typically, these materials consist of sub-wavelength metallic inclusions embedded within or on top of a dielectric matrix or substrate material. A great deal of research into metamaterials has used microwave radiation due in part to the ease of fabrication of sub-wavelength structures at these frequencies. For example demonstrations of negative refractive index media composed of negative permittivity (ε) and negative permeability (μ) metamaterial elements was first demonstrated at microwave frequencies [3]. This has led to intense efforts to extend metamaterial response to terahertz ($1\text{THz}=10^{12}\text{Hz}$) [6], near-infrared, and visible frequencies [7-9]. Thus, these designer materials not only extend and complement natural material response; they have also been demonstrated over a significant portion of the electromagnetic spectrum.

Although most effort in metamaterials research is advancement to optical frequencies, some work has concentrated on THz frequencies [6, 10, 11]. There are many potential uses for metamaterials specifically within this regime, as response from naturally occurring materials is somewhat rare and there is a noticeable lack of high power

*raveritt@physics.bu.edu; phone 617 353-2619; fax 617 353-9393

Terahertz Physics, Devices, and Systems II,
edited by Mehdi Anwar, Anthony J. DeMaria, Michael S. Shur,
Proc. of SPIE Vol. 6772, 677209, (2007) · 0277-786X/07/$18 · doi: 10.1117/12.751613

sources, efficient detectors, and other standard device components.

Metamaterials yield resonant electromagnetic behavior where the range of the frequency response is set rigorously by their geometry and constituent permittivity. For some applications a narrow bandwidth is desirable while for others a broader bandwidth is required which presents distinct challenges. Also, for many potential applications, it would be desirable to create metamaterials that exhibit an externally controlled active, dynamical, and/or tunable response. Thus, the terahertz frequency regime is a rich area to study potential metamaterial based devices owing to the lack of naturally occurring materials and the possibility of high payoff. In addition, terahertz wavelengths (1 THz → 300 μm) are such that standard photolithography can be employed to fabricate subwavelength elements.

In this paper we present two metamaterial based devices operating at THz frequencies. First, we demonstrate the potential for a split ring resonator (SRR) structure fabricated on a semiconductor to switch/modulate electromagnetic radiation via optical doping of the substrate. We also present an efficient active metamaterial based Schottky diode switch / modulator which enables all electronic voltage control of the MM response. Terahertz time domain spectroscopy is used to characterize both materials and we supplement the experimental findings with results from finite element simulations to investigate the underlying physics and performance of both device responses.

2. PLANAR METAMATERIALS ON SEMICONDUCTING SUBSTRATES

2.1 Planar Electrical Metamaterials

Similar to the magnetic resonance using split ring resonators (SRRs), metamaterials can also be designed to exhibit a purely electric resonant response [12-14]. Figure 1(a) shows an example unit cell of a planar metamaterial composed of electric split ring resonators (eSRRs). It is based on symmetric design, i.e., two SRRs are configured face to face. The electric field of the incident electromagnetic waves drives the counter-circulating currents, in which the opposite magnetic dipoles are cancelled. The purely electric resonant response is shown in Fig. 1(c) that is the result of finite-element numerical simulation. The structure dimensions (described in Fig. 1) are chosen such to yield a resonant response at THz frequencies. They are periodically patterned in a planar square array on a semi-insulating gallium arsenide (SI-GaAs) substrate by photolithographic methods. The metallization consists 200 nm thick gold following

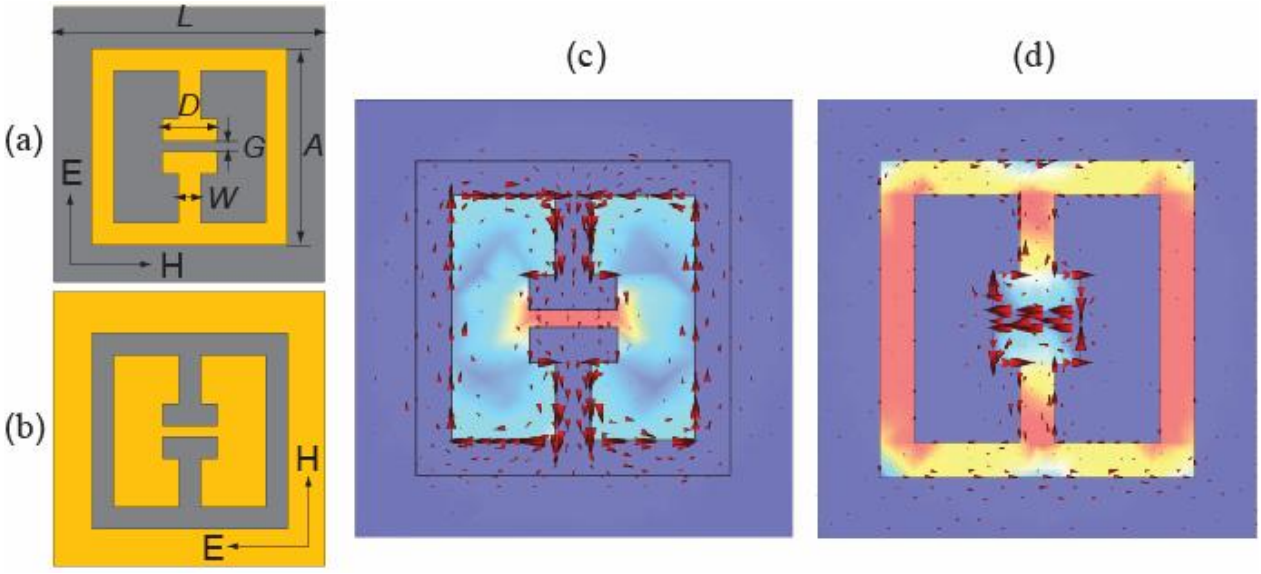

Figure 1: (a) and (b) unit cell structures of the original and complementary metamaterials. (c) and (d) the corresponding surface current flow (arrows) and electric field norm (color mapping) of the original and the complementary metamaterials. The structure dimensions are: A = 36 μm, G = 2 μm, D = 10 μm, W = 4 μm, and the lattice parameter L = 50 μm.

10 nm thick titanium as adhesion layer by electron beam deposition. We also fabricate the inverse structure termed

"complementary" metamaterial as shown in Fig. 1(b). In contrast to the magnetic response [15], it also exclusively shows purely electric resonant response as indicated by the numerical simulation shown in Fig. 1(d).

A THz time domain spectroscopy system is used to characterize the metamaterial samples. The polarization of normally incident impulsive THz radiation are configured as the dual sources in accordance with the Babinet's principle, as shown in Fig. 1(a) and (b). The THz electric field transient is measured in the time domain after propagating through the metamaterial sample, and through a bare SI-GaAs as a reference. The Fourier transformed samples spectra divided by the reference spectrum give us the complex transmission from which the amplitude and phase can be simultaneously obtained. This further permits the extraction of the effective complex dielectric function of the metamaterials using the inversion of the appropriate Fresnel equations.

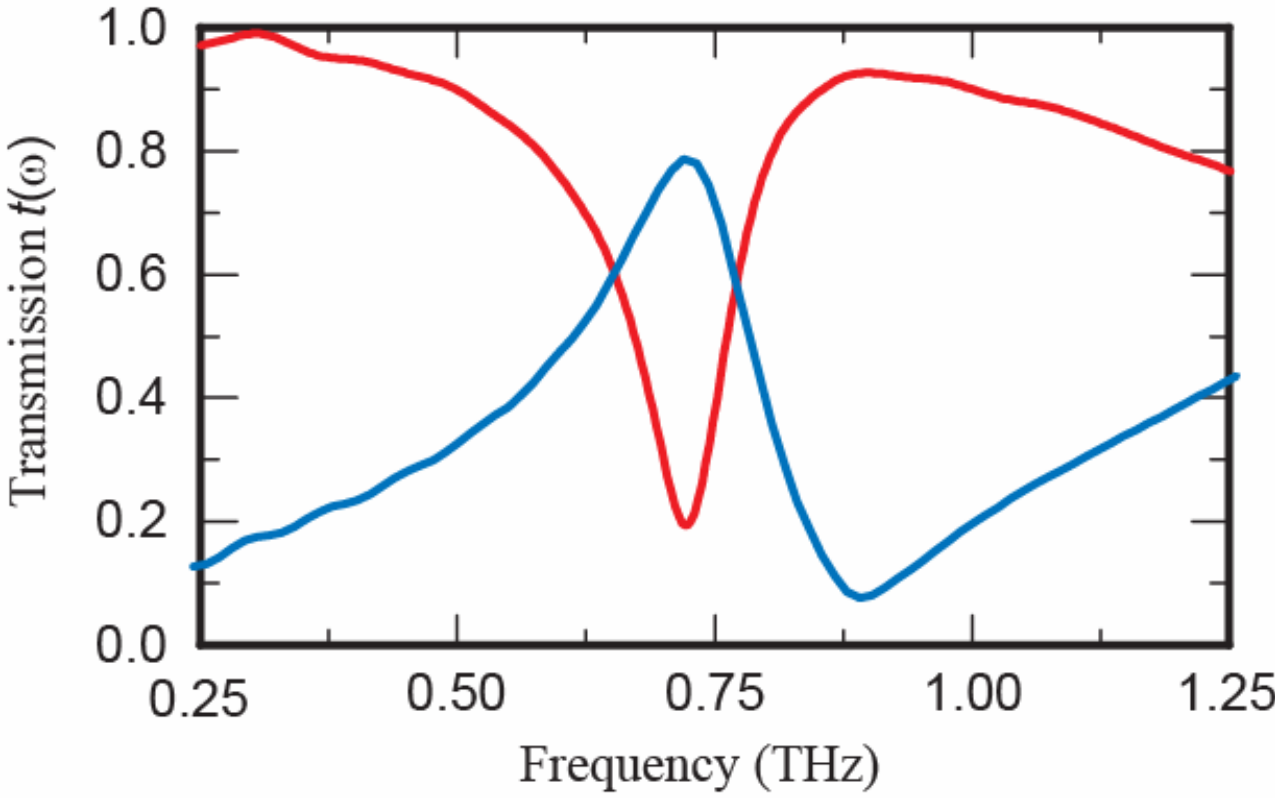

Figure 2: Transmission of THz electric field amplitude for the original (red curve) and the complementary (blue curve) metamaterials.

The frequency dependent transmission amplitude of the THz electric field is shown in Fig. 2. They are in excellent agreement with the numerical simulations (not shown). In the original metamaterial at resonance, the normally incident THz electric field induces an array of electric dipoles at the split gaps, which reradiates and destructively interferes with the indicent THz radiation thereby giving the THz transmission minimum at ~0.7 THz. In the complementary metamaterial, while off-resonance, most of THz radiation is blocked by the large metallic coverage. At resonance, however, the induced electric dipole array reradiates and results in a THz transmission maximum. The THz transmission minimum and maximum in the original and complementary metamaterials occur at the same frequency, and furthermore, the sum of the transmission amplitudes is close to one, which is in good agreement with the Babinet's principle. The resonances result in negative values of effective dielectric constant in the original metamaterial, and positive values in the complementary metamaterial despite the Drude-like response due to the large coverage of metal film [15]. Thus, we see that it is possible to create metamaterials at terahertz frequencies with a specific response. In the following section we discuss the properties of the substrate upon which the metamaterials are fabricated as this provides a route towards controlling the electromagnetic response. The subsequent two sections will, respectively, detail our results on the optical and voltage control of the metamaterial response.

2.2 Substrate Considerations

The substrate upon which a metamaterial is fabricated is important beyond simply providing mechanical support. Conventionally, it is desirable to minimize substrate losses and to account for the redshift (in comparison to a free standing structure) of the resonant response due the real part of the substrate dielectric response. However, the ability to tune the dielectric response of the substrate $\varepsilon(\omega) = \varepsilon_{s1} + i\varepsilon_{s2}$ provides the means to dynamically control the resonant MM response. Specifically, changes in ε_{s1} enable tuning of the metamaterial resonant frequency ω_0 while changes in the real part of the substrate conductivity $\sigma_{s1} = \omega\varepsilon_0\varepsilon_{s2}$ modifies the magnitude of the MM resonance. In the following, we will only consider dynamic and active control of the magnitude of the MM response via changes in the substrate conductivity as obtained by modification of the carrier density using photo-doping or voltage controlled carrier depletion.

The metamaterial structures introduced above and in the following are fabricated on semiconducting substrates. This includes (i) semi-insulating Gallium Arsenide (SI-GaAs) and (ii) GaAs:ErAs nanoisland superlattices for photo-doping and (iii) a thin n-doped GaAs layer to create a Schottky diode structure thereby offering control via a voltage bias. Further details are discussed below.

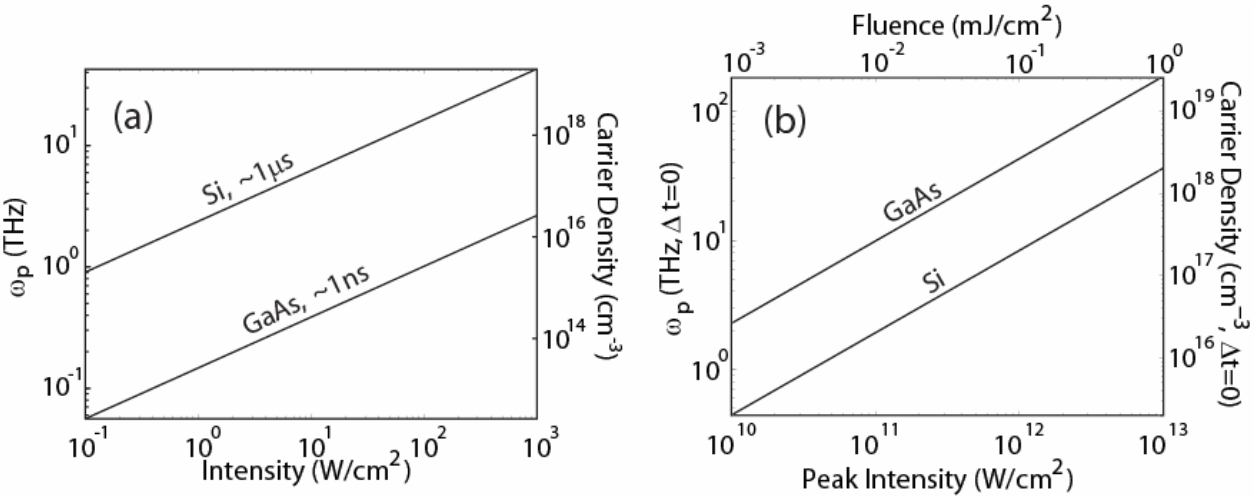

Figure 3: (a) Calculated carrier density and plasma frequency as a function of intensity in Si and GaAs for CW excitation. (b) Peak carrier density and plasma frequency for ~100 fs excitation.

A general consideration for carrier density control of MM is the absolute value of the carrier concentration. If the substrate carrier concentration is too large, the sample will have near unity reflectivity whereas too small of a carrier density will not enable control of the metamaterial resonance. Specifically, the density must be large enough such that the plasma frequency $\omega_p^2 = ne^2/\varepsilon_0 m$ is greater than ω_0. Clearly, the larger ω_0 the larger the carrier density required making such an approach for carrier density control at say, near-IR or optical wavelengths, difficult. In contrast, at THz frequencies fairly low carrier densities (~10^{16}cm^{-3}) are sufficient to control the MM response as shown below.

Finally, we mention that for optical control of MM, the carrier generation efficiency must be considered. The number of carriers generated (per cm^3) is given by

$$n = 6.25\times10^{18}\frac{I_0(1-R)\tau}{Ad\hbar\omega}$$

where I_0 is the average power in Watts, R is the reflectivity, $\hbar\omega$ is the photon energy in eV, A is the area of the laser excitation, and d is either the penetration depth or sample thickness in the appropriate limit. This expression is valid for CW and pulsed excitation. For CW excitation, τ is the recombination time while for short pulse excitation, τ is the repetition period of the laser where it is assumed that the pulse duration and pulse repetition period are much less than the carrier recombination time. Figure 3 shows simple calculations for CW and short pulse excitation (at 800 nm) for Si

and GaAs. For CW excitation, Si yields a larger carrier density for a given intensity because of the longer recombination time. In contrast, for pulsed excitation GaAs yields a larger carrier density for a given peak intensity because of the shorter penetration depth. The value of ω_p provides the upper limit for controlling the MM response. At THz frequencies quite low intensities can be utilized whereas considerably higher intensities are required at higher frequencies presenting a practical limitation of carrier density control of the MM response (at least using a Drude-like response).

3. OPTICAL CONTROL OF METAMATERIALS

The electromagnetic response of the SRR metamaterial fabricated on SI-GaAs is shown in Fig. 4. We show the transmitted electric field as a function of frequency in Fig. 4(a) and the corresponding dielectric function $\varepsilon_1(\omega)$ in Fig. 4(b). Let us focus on the steady state response of $T(\omega)$ with no optical excitation, shown as the solid black curve in Fig. 4(a). At low frequencies $T(\omega)$ is relatively high with values near 95%. Near 0.5 THz the transmission drops to ~20% and then recovers back to 95% by 0.75 THz. This attenuation of transmission is associated with the circulating resonance of the SRR, as verified by the numerical simulations shown in Fig. 1 of ref. [11]. This low energy THz resonance, due to an electric response $\varepsilon(\omega)$ of the SRRs, occurs at the same frequency as the magnetic $\mu(\omega)$ resonance. Continuing to higher frequencies the SRR metamaterial yields another resonant feature in $T(\omega)$ near ω_1 = 1.6 THz. This dipolar resonance is addressed in detail in ref. [11] and we do not discuss this further.

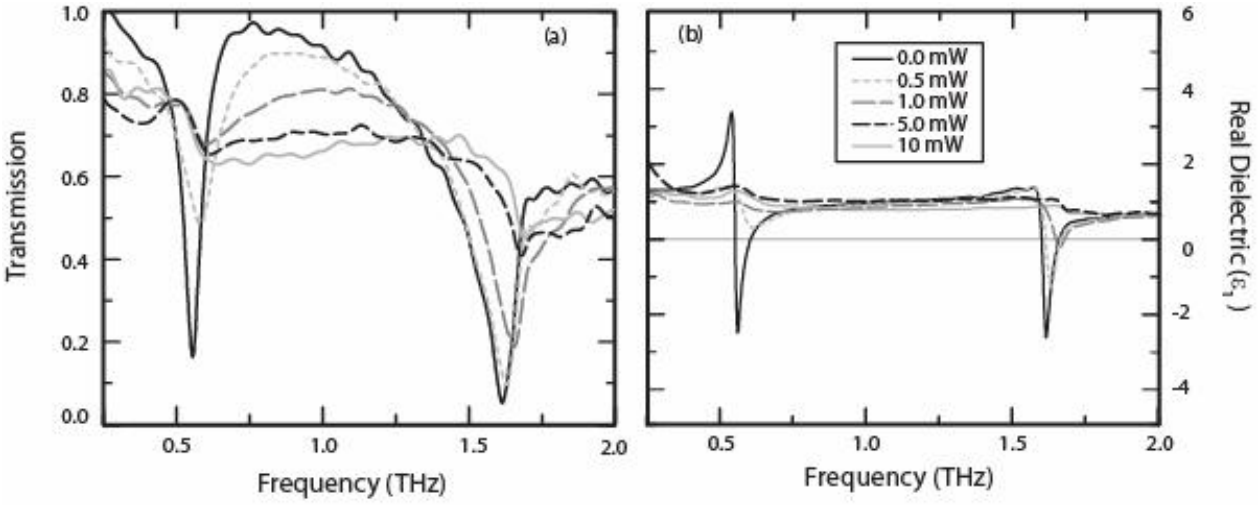

Figure 4: (a) Transmission spectra as a function of photo-doping fluence for the electric resonance of the SRRs. The polarization of the incident EM wave is perpendicular to the gap. As the power is increased ω_0 is shorted out and the overall transmission decreases. At higher powers ω_1 can also be seen to die off. (b) Corresponding change of the real dielectric constant $\varepsilon(\omega)$ of the SRRs as a function of power.

The results of uniform optical excitation the SRR metamaterial array with 800 nm light at increasing for various incident optical power is shown Fig. 4. Since we utilized optical pump THz probe spectroscopy, we time our excitation pulse, (50 fs width), to occur at t=-5ps before our THz pulse. This will ensure there is a well established steady state population of photocarriers, since the lifetime of carriers in SI-GaAs is significantly longer than the duration of the THz pulse. SRRs have been shown to strongly focus electric fields within the split gap of the structure. Thus, the resonant properties of the metamaterial, and hence the electromagnetic response of the entire device is largely governed by the properties of materials within the gap. The photo-generated free carriers should act to short circuit the gap of the SRR and eliminate the resonant properties, restoring higher values of $T(\omega)$. In Fig. 4(a) we show the dependence of $T(\omega)$ on pump power. At a pump power of 0.5 mW (dashed gray curve of Fig. 4) the transmission changes drastically and increases by nearly a factor of three to 50% at resonance. Notice however that outside the range of this resonance, the transmission has only a slight decrease in value. We determined that a pump power of 0.5 mW corresponds to a fluence of 1 $\mu J/cm^2$ or equivalently to a photoexcited carrier density $n \sim 2X10^{16} cm^{-3}$. Notice that although the lower frequency resonance near 0.5 THz has had drastic changes under optical excitation of 0.5 mW the higher frequency dipolar resonance at 1.6 THz

has undergone little change. However at increased pump powers (1 mW (n ~ $2X10^{16}cm^{-3}$)) the low energy resonance is nearly entirely eliminated and the higher energy resonance decreases as well. These trends continue and finally at 5 mW of pump power both resonance are quenched and the transmission is relatively frequency independent.

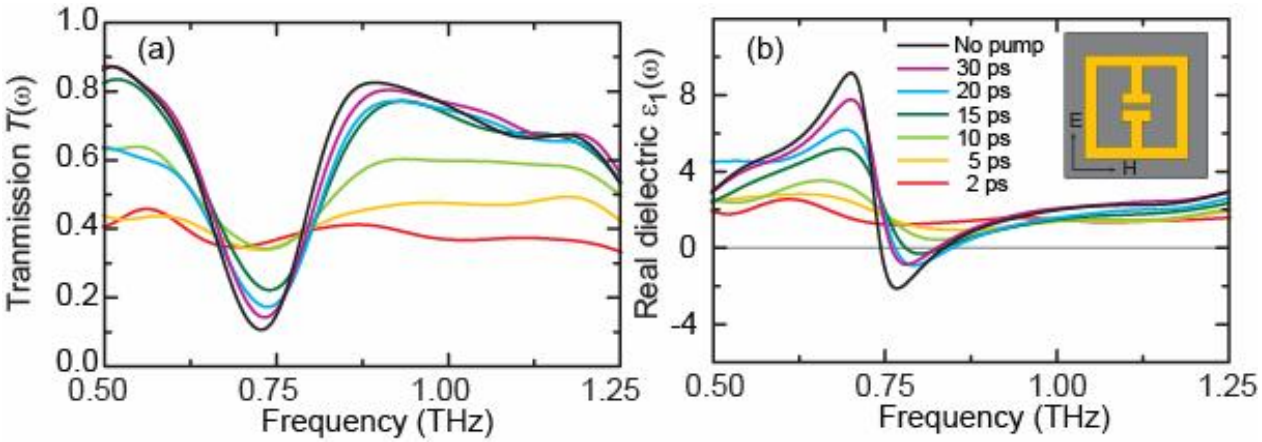

Figure 5: (a) MM transmission spectra at various times following photoexcitation of carrier in the ErAs:GaAs nano-island substrate. (b) Corresponding real permittivity.

As mentioned, measurement of the time dependence of the transmitted electric field permits calculation of the optical constants and we now shift discussion to the real part of $\varepsilon_1(\omega)$ as a function of excitation power, displayed in Fig. 4 (b). Both resonances yield a Lorentz-like frequency dependent form, with no pump excitation, in $\varepsilon_1(\omega)$ as can be seen in Fig. 4 (b). Notice further that in the vicinity of both resonances that the dielectric function obtains negative values. The region of negative $\varepsilon_1(\omega)$ achieves 9% and 5% bandwidths for the lower and higher frequency resonances respectively. For a pump power of 0.5 mW the lower energy resonance is reduced greatly and the $\varepsilon<0$ response vanishes.

For MM fabricated on SI-GaAs, switching off the resonance occurs within 5 ps. However, the recovery time is dictated by the recombination time of the carriers which, as mentioned above, is approximately 1 ns. This long recovery time clearly limits the duty cycle for switching the MM resonance. A simple way to improve the on/off times is to fabricate the planar array on a material with a short carrier lifetime. We have utilized ErAs:GaAs nanoisland superlattices to reduce the carrier lifetime. Essentially, ErAs nanoparticles trap the carriers and the lifetime can be controlled through the spacing between adjacent ErAs nanoparticle layers. For the purposes of demonstration, our ErAs:GaAs samples were fabricated with a layer spacing of 100nm resulting in a lifetime of 10ps. In principle, the carrier lifetime can be less than 1ps by reducing the layer spacing, but this would be too fast to appropriately analyze the MM response using simple one dimensional OPTP. Figure 5(a) shows the MM transmission as a function of frequency at various times following excitation with a fluence of 2 $\mu J/cm^2$ and Fig. 5(b) displays the corresponding effective real dielectric response. The resonance is switched off within 2ps and fully recovers within 15 ps consistent with the carrier lifetime. These results show that it is possible to create ultrafast terahertz modulators using planar MM arrays opening possibilities for high bit rate communication at THz frequencies [15].

4. VOLTAGE CONTROLLED METAMATERIALS

In this section, we describe a high efficient electrically switchable THz metamaterial device. As described above, the principle is that the implemention of semiconductor structures into metamaterial substrate enables modification of the capacitive split gaps and/or the inductive loops, thereby tuning the resonance strength and/or the resonance frequency. Fig. 6 shows a schematic design of such an active THz metamaterial device [16]. We fabricate the planar metamaterial on GaAs substrate, which has a 1 μm thick n-doped layer with free carrier density $1.9X10^{16}cm^{-3}$ on top of SI-GaAs substrate. The all-connected metallic metamaterial elements and the doped semiconductor layer form a Schottky structure, in which the depletion width can be actively tuned by applying a reverse bias voltage. The metamaterial is as

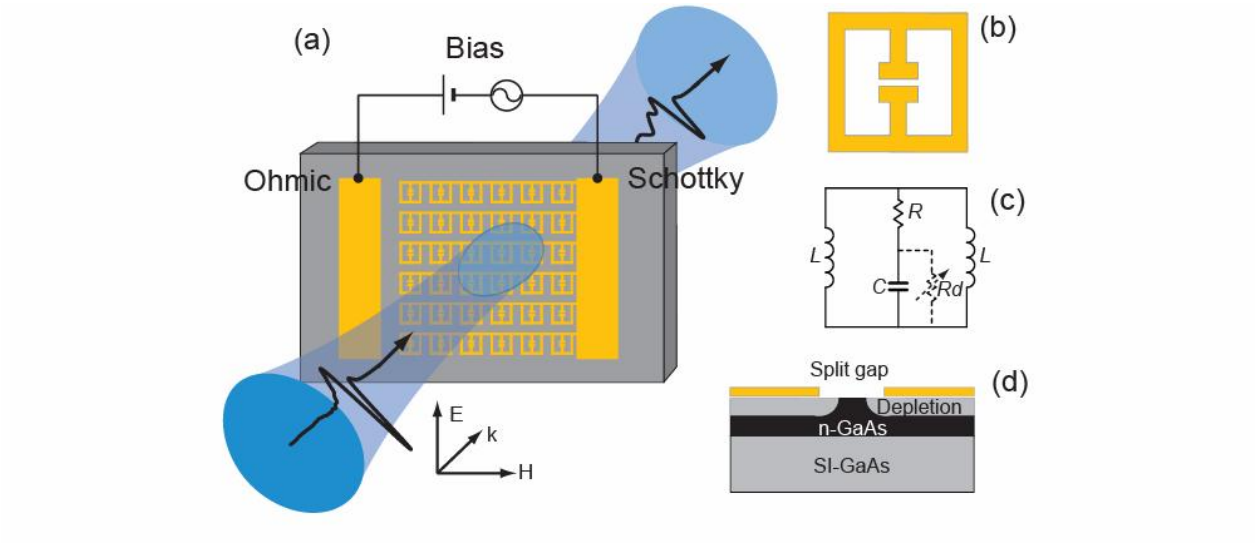

Figure 6: Electrically switchable THz metamaterial device. (a) Schematic of THz metamaterial device and experimental measurements. (b) electric split ring resonator. (c) Equivalent circuit where the dashed variable resistor indicates the leakage of substrate. (d) Diagram of the substrate and the depletion region near the split gap.

above - metallized 200 nm gold with 10 nm titanium as an adhesion layer created using photolithographic methods and electron beam deposition. The ohmic contact is fabricated by electron beam deposition of 20 nm germanium, 20 nm nickel, and 150 nm gold, then performing rapid thermal annealing at 350 ^{o}C for 1 min.

We perform THz transmission measurements with the THz electric field polarization indicated in Fig 1(a). With no voltage bias, the relatively conducting substrate results in a leakage current that can easily damp the resonance. This is shown by the black curve in Fig. 7. An increasing reverse voltage bias increases the depletion width and isolates the metallic metamaterial from the conductive substrate, thereby restoring the resonance. This is shown by the results in Fig. 7. The results also indicate that, because of the symmetric design of the eSRRs, the connecting wires do not affect the resonance. By this approach, we are able to effectively switch the metamaterial resonant response, and the THz transmission with efficiency up to 50%, by applying an electrical voltage bias. Furthermore, the effective dielectric constant near resonance can be switched between positive (no resonance) and negative (strong resonance) values [16].

In order to define the switching speed and modulation performance, we measure the modulation (differential) THz signal by applying a reverse square voltage bias alternating between 0 and 8 volts. Fig. 8 shows the results. We found that upon increasing the modulation frequency, the modulation efficiency significantly decreases, though at 100 kHz the THz modulation signal is still observable. These results are not surprising since we have a large device area (5mmX5mm) that gives a large device capacitance underneath the metallic metamaterial and the low doping level gives the series resistance, which results in an *RC* roll-off. Further improvements such as patterning the doping regions just near the split gaps and/or using interdigited ohmic electrodes, or the use of other semiconductor structures should significantly improve the performance.

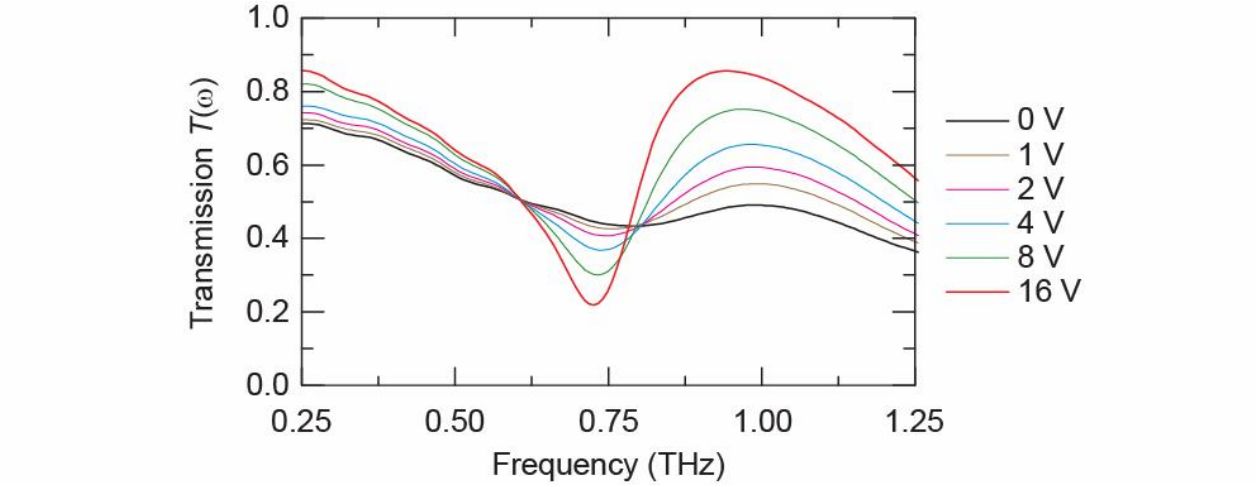

Figure 7: THz transmission of intensity versus frequency for various applied reverse voltage bias.

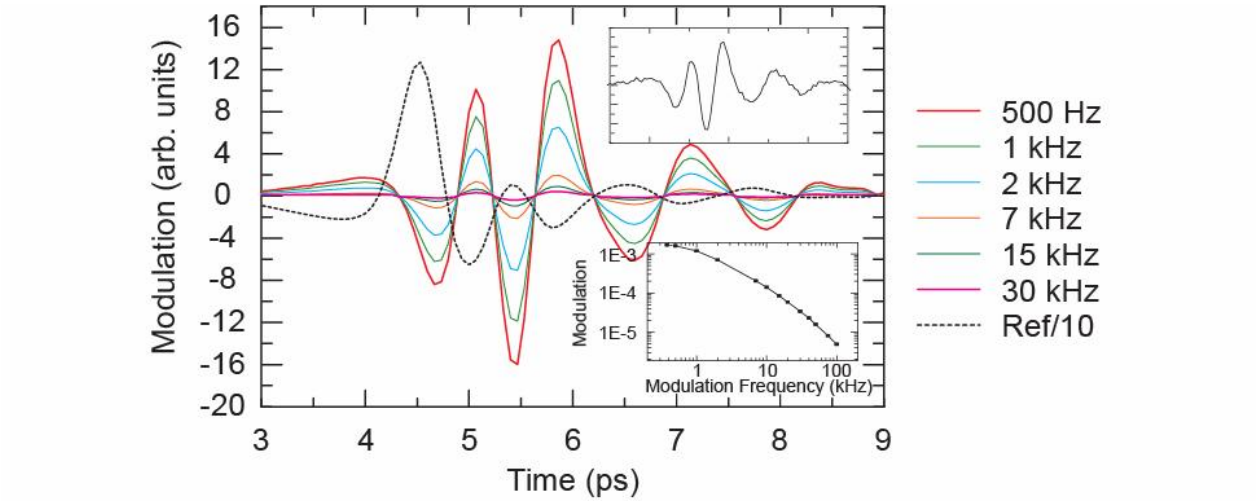

Figure 8: THz modulation (differential) signal under various frequency of the reverse square voltage bias alternating between 0 and 8 volts. The dashed black curve is as transmitted THz signal as a reference without voltage bias. The top inset is the THz modulation signal at 100 kHz; the bottom inset shows the relative modulation signal as a function of frequency.

In summary, we have demonstrated that it is possible to design metamaterials with a specific electromagnetic response at terahertz frequencies, and that it is possible to control this resonant response using both optical and electronic approaches.

Acknowledgement: The authors would like to thank Kevin Baldwin for his technical help on the sample fabrication. We also acknowledge support from the Los Alamos National Laboratory Laboratory Directed Research and Development Program. This work was performed, in part, at the Center for Integrated Nanotechnologies, a U.S. Department of Energy Office of Basic Energy Sciences nanoscale science research center operated jointly by Los Alamos and Sandia National Laboratories.

REFERENCES

1. Pendry, J. B.; Schurig, D.; Smith, D. R., Controlling electromagnetic fields. *Science* **2006,** 312, 1780-1782.

2. Schurig, D.; Mock, J. J.; Justice, J. B.; Cummer, S. A.; Pendry, J. B.; Starr, A. F.; Smith, D. R., Metamaterial electromagnetic cloak at microwave frequencies. *Science* **2006,** 314, (977-980).

3. Shelby, R. A.; Smith, D. R.; Schultz, S., Experimental verification of a negative index of refraction. *Science* **2001,** 292, 77-79.

4. Smith, D. R.; Padilla, W. J.; Vier, D. C.; Nemat-Nasser, S. C.; Schultz, S., Composite medium with simultaneously negative permeability and permittivity. *Physical Review Letters* **2000,** 84, 4184-4187.

5. Fang, N.; Lee, H.; Sun, C.; Zhang, X., Sub-diffraction-limited optical imaging with a silver superlens. *Science* **2005,** 308, 534-537.

6. Yen, T. J.; Padilla, W. J.; Fang, N.; Vier, D. C.; Smith, D. C.; Pendry, J. B.; Basov, D. N.; Zhang, X., Terahertz Magnetic Response from Artificial Materials. *Science* **2004,** 303, 1491-1496.

7. Dolling, G.; Enkrich, C.; Wegener, M.; Soukoulis, C. M.; Linden, S., Simultaneous negative phase and group velocity of light in a metamaterial. *Science* **2006,** 312, 892-894.

8. Yuan, H. K.; Chettiar, U. K.; Wenshan, C.; Kildishev, A. V.; Boltasseva, A.; Drachev, V. P.; Shalaev, V. M., A negative permeability material at red light. *Opt. Express* **2007,** 15, 787207877.

9. Zhang, S.; Fan, W.; Panoiu, N. C.; Malloy, K. J.; Osgood, R. M.; Brueck, S. R., Optical negative-index bulk metamaterials consisting of 2D perforated metal-dielectric stacks. *Opt. Express* **2006,** 14, 6778-6787.

10. Azad, A. K.; Zhang, W., *Opt. Lett.* **2005,** 30, 2945.

11. Padilla, W. J.; Taylor, A. J.; Highstrete, C.; Lee, M.; Averitt, R. D., Dynamical electric and magnetic metamaterial response at terahertz frequencies. *Physical Review Letters* **2006,** 96, 107401/1-4.

12. Padilla, W. J.; Aronsson, M. T.; Highstrete, C.; Lee, M.; Taylor, A. J.; Averitt, R. D., Novel Electrically Resonant Terahertz Metamaterials. *Phys. Rev. B, Rapid* **2007,** 75, 041102.

13. Schurig, D.; Mock, J. J.; Smith, D. R., *Appl. Phys. Lett.* **2006,** 88, 041109.

14. Chen, H. T.; O'Hara, J. F.; Taylor, A. J.; Averitt, R. D.; Highstrete, C.; Lee, M.; Padilla, W. J., Complementary planar terahertz metamaterials. *Opt. Express* **2007,** 15, 1084.

15. Chen, H. T.; Padilla, W. J.; Zide, J. M. O.; Bank, S. R.; Gossard, A. C.; Taylor, A. J.; Averitt, R. D., Ultrafast optical switching of terahertz metamaterials fabricated on ErAs/GaAs Nanoisland Superlattices. *Opt. Lett.* **2007,** 32, 1620-1622.

16. Chen, H. T.; Padilla, W. J.; Zide, J. M. O.; Gossard, A. C.; Taylor, A. J.; Averitt, R. D., Active terahertz metamaterial devices. *Nature* **2006,** 44, 597-600.